# DIRECT PORE-SCALE MODELING OF TWO-PHASE FLOW THROUGH NATURAL MEDIA

I.I. Bogdanov[*,1], F. Guerton[2], J. Kpahou[1,2] and A.M. Kamp[1]
1) Open & Experimental Centre for Heavy Oil, University of Pau, Pau, France
2) Laboratory of Complex Fluids and Their Reservoirs, University of Pau, Pau, France
*Corresponding author: UFR Sciences et Techniques – avenue de l'Université – bât. B1 – BP 1155 - 64013 Pau France; email: igor.bogdanov@univ-pau.fr

**Abstract:** Pore-scale modeling of multiphase flow of petroleum reservoir fluids through real natural porous media is a true challenge for engineering and scientific society. Because the pore-scale description is a fundamental approach in hydrodynamics it is addressed most frequently to improve our understanding of flow and transport phenomena in such settings. Besides, it can be used to obtain macro-scale constitutive equations, to provide multiphase flow properties for large scale models, to predict how these properties may vary with rock type, wettability etc.

One of the important aspects of this problem is the construction of adequate 3D numerical models of flow through pore space. With the recent development of computed micro-tomography (μCT) technique it becomes evident that direct numerical simulations (DNS) at pore-scale will be widely used in the porous medium modeling and particularly, in petroleum applications. The geometrical description of flow region via X-ray μCT, the generation of a 3D grid in real pore space and the corresponding flow computations, constitute the principal objective of our current work. For a simulation of fluid distribution inside pores the models based on incompressible Navier-Stokes equations and their extension to diffuse interface (Cahn-Hilliard) model are used.

Transport properties for single- and two-phase flow, stationary and transient flow patterns at various viscosity ratio and capillary numbers, the offset of the displacement instability, numerical performance of diffuse interface model in a specific 3D framework, are presented and discussed in some details.

The developed methodology of a porous medium properties computation is a valuable tool for both fundamental porous medium and applied petroleum and environmental applications.

**Keywords:** direct numerical simulation, multiphase flow, real pore geometry, computed micro-tomography, diffuse interface.

## 1. Introduction

The fast and continuous development of computers power, architecture and computational performance gives rise to the problem formulations and solution approaches which until recently seemed to be inappropriate for practical use.

Among them were direct numerical simulations (DNS) and/or measurements of flow in real pore space. During decades the direct pore-scale modeling (PSM) was frequently considered impossible and therefore senseless because the flow fields could not be reliably observed and measured at this scale (cf. Bear, 1988; chapter 1) and thus could not provide any meaningful information.

Note that during decades that was true in many situations. However, currently the numerical simulations coupled with laboratory measurements get back more and more to the pore-scale description which is a fundamental approach in hydrodynamics. (We'll use hereafter a term "pore-scale" and not "micro-scale" to distinguish between them as the notion "microscopic point" defined, for instance, by Bear, 1988, refers to a REV scale containing by definition numerous pores). This approach is often addressed or mentioned when there is a need to improve our understanding of transport phenomena in such settings. It may provide valuable information about some principle theoretical notions underlying conventional flow models. Besides, it can be used to obtain macro-scale constitutive equations, to provide single- and multiphase transport properties for large scale models, to predict how these properties may vary with rock type, wettability etc.

The precise geometrical characterization of void space in natural materials becomes a key issue. Resulting from improved software and measurements technique, the recent advances in X-ray μCT allowed greater access to both higher resolution and volume of porous samples, and to a larger set of information useful in the porous media flow modeling. The range of energies used in the X-ray tomography allows a study of very dense

objects, such as rocks. The X-ray attenuation depends on the chemical composition of the material and its physical density. This µCT technique gives a unique opportunity for non-destructive 3D core sample insight. An example of a porous cubic sample acquired via µCT is shown in figure 1. So the geometrical description of flow region via µCT imaging, the generation of a 3D grid in a real pore space, the discretized numerical model associated with this grid and the adequate flow computations, constitute the principal objective of our current work. For a computation of fluid distribution inside pores the models based on incompressible Navier-Stokes equations and their extension to diffuse interface (Cahn and Hilliard, 1958) model are used.

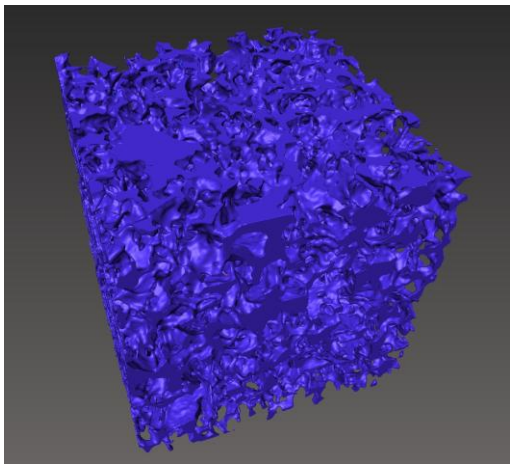

**Figure 1**. Example of a porous sample acquired via µCT and image processed, (500 slices stack, Bentheimer rock); $L \approx 2.5$mm.

## 2. Micro-tomographic imaging of a real porous medium

Prior to extract, via a dedicated image processing software, necessary data and the geometrical description of the connected and unconnected porosities inside the sample, a tomographic acquisition of the later has to be carried out. We use a Skyscan 1172 µCT device to analyze our samples. As first step, the sample is fixed on a stepping motor motorized holder; the apparatus takes side view projections of the sample. At 0.3° angular step acquisition, more than 600 projections are required and recorded. As second step, the recorded projections are processed via a Feldkamp-like algorithm to reconstruct slice by slice a virtual sample. Each slice is a 2D 16 bits TIFF grayscale picture. The slice pictures stack depicts the whole 3D sample.

After that the image processing on the slice stack is required. This step is very sensitive to setting parameters. We choose to study a well documented rock, the Bentheimer sandstone, in order to tune this image processing step on referenced values.

On the grayscale pictures stack image processing is made using Avizo software (Fire edition, VSG company). To measure the porosity from the processed picture slices, a *Volume 3D Filter* is applied on the stack. For Bentheimer sansdstone, the average porosity is $0.21 \pm 3\%$ while a value of $0.207 \pm 1.5\%$ was calculated from our tests.

## 3. Geometrical description and image based grid generation

To estimate numerically the sample transport properties, isolated pores (non-connected to the main pore network) have to be deleted before meshing. Via an *Individual Analysis* measurement tool, the connectivity is investigated by labeling each pore, the pore volume and surface are also measured and only the main porosity is kept. A *Not Filter* is applied on the whole stack to code the binary pictures: porosities are now depicted as a bulk and can be meshed. For visualization, a surface generation tool could be applied on the stack.

The result is exported as a set of TIFF pictures in a dedicated software, ScanIP (SimpleWare company), for triangulation of pore space total surface. ScanIP provides a robust approach for the conversion of stack of binarized (or labeled) images into surface meshes.

To reduce the size of the grid (which could be memory and time consuming) we used *Resampling* and *Cropping* tools prior to the mesh generation. Note that *Resampling* does not modify an object size but reduced (sometimes, significantly) the total number of geometrical elements. This step may be somewhat critical because it may modify the connectivity, and hence the transport properties (for example, small throat between pores could be removed). The *Cropping* tool is used to reduce the model volume: a subregion of interest has to be chosen, which is inside the stack in size and location. This cutting process can isolate some pores from the main network (as the new boundaries have been generated). Therefore a *Kill Border Filter* has to be applied on the new volume in order to remove

these unconnected porosities. Notice that the *cropped* "sample" is to be "representative" which may be a problem because of reduction in the sample size.

For each object the triangular mesh was generated first. Then the surface meshes were imported as geometry file into COMSOL *Multiphysics* 4.2 for direct numerical simulations of pore-scale single- and two-phase (hereafter 1P and 2P, respectively) flow patterns. As a rule the volume (tetrahedral) grid was done using COMSOL and required rather fine discretization to get reliable results even for single-phase flow computations.

## 4. Flow computations

The stationary (mainly, 1P) and transient 2P flow regime calculations were done making use of Navier-Stokes and Cahn-Hilliard pore-scale models, respectively (Cahn and Hilliard, 1958; see also Appendix below). The corresponding numerical problem formulations and general results are discussed below.

To optimize the computational expenses the initial sample (figure 2) has been *cropped* into 8 regular cubs of equal volume. For each cube (or in other word, each $1/8^{th}$ of sample; cf. figure 3) the porosity and the absolute permeability have been calculated. Their directional (i.e. x-, y- and z-direction) flow rate and total pore volume (porosity) variation for different $1/8^{th}$s turned out to be relatively small so that the original sample can be taken as uniform at the scale of few tens of pores.

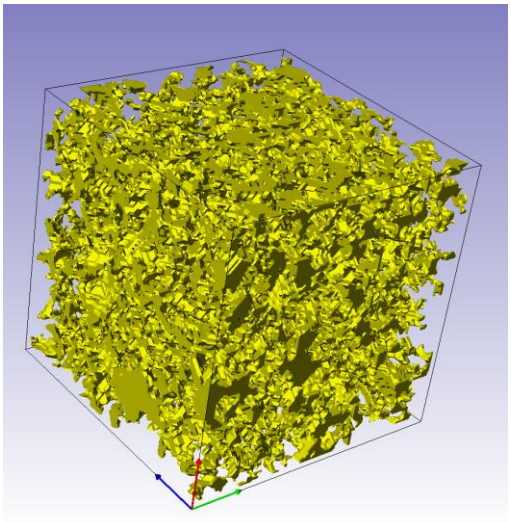

**Figure 2**. Original Bentheimer sandstone sample after reconstruction in ScanIP; $L$=2.45mm (cf. figure 1).

### 4.1. Grid generation

One of the most important components for successful numerical pore-scale model (both in 1P and 2P cases) is an adequate choice of tetrahedral grid. By now all grids used in our work were generated in COMSOL with the use of local grid refinement towards grain surfaces ("*Fluid Dynamics*" built-in mesh generation option). Usually, the complicated geometry of pores and channels (figures 2 and/or 3) taken from reconstructed images without intermediate processing (smoothing), was prohibitive for generation of relatively coarse grid. In practice, a half of generated grids were done at "fine" or even "finer" level (in terms of COMSOL internal grid definitions). One of the most small grid examples shown in figure 3, contains approximately $2 \cdot 10^5$ of grid elements, the worst element quality being of order of 0.1.

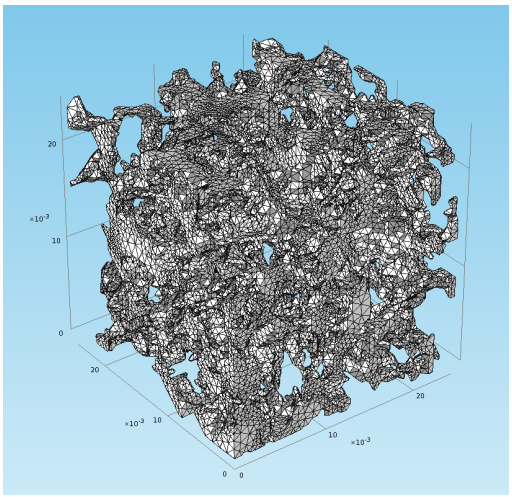

**Figure 3**. One eighth of original Bentheimer sample: geometry and mesh; $L_1=L/2$ (cf. figure 2).

### 4.2. Single-phase flow properties

The porosity and absolute permeability are addressed in this study. The dimensionless Navier-Stokes equations at Darcy limit (global Reynolds number meets $Re << 1$) describe laminar flow regime. It doesn't mean however that no other information is available in a 1P flow simulation results. While the porosity computation is still straightforward and in principle is available in earlier stage of image processing, the absolute permeability (i.e. total flow through a sample) determination required more advanced procedure of flow simulation. It will generally depend on lateral boundary

conditions (and so, on the sample shape) and pore-space topology. The roughness (or equally, smoothness) of grain surfaces which can hardly be measured at the moment, may be an important parameter together with 3D channels tortuosity. The latter can be modeled numerically (Fourie et al, 2007, cf. also figure 4) and/or measured experimentally using any known procedure, for instance, based on tomographic reconstruction images.

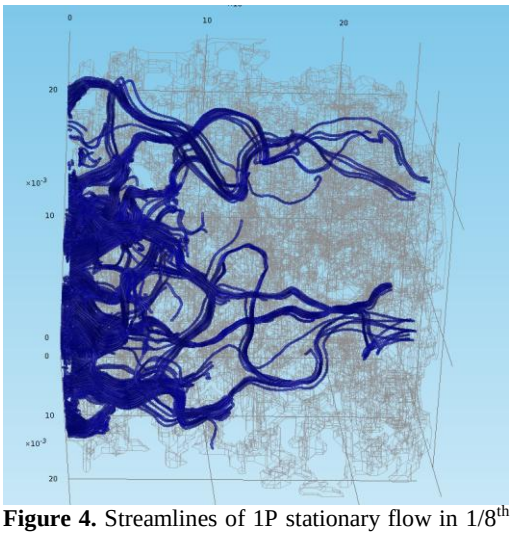

**Figure 4.** Streamlines of 1P stationary flow in 1/8$^{th}$ of original sample (figure 3); flow direction is from left to right.

Single-phase flow transport properties may be computed first from steady-state 3D flow problem solution and then compared to experimental data. To obtain numerical results the *Incompressible Navier-Stokes* application mode has been used for modeling. Special care has been taken to provide necessary mass balance in pore volume and laminar flow regime. Low enough Reynolds numbers can be controlled via imposed pressure drop between the inlet and outlet faces of a cubic sample. Note that even at these conditions the local velocity field is far from being smooth and regular (figure 5, shown in the figure are velocities in the range $2\cdot10^{-7}\div6\cdot10^{-4}$ m/s). Different boundary conditions on lateral sides (no-slip, symmetric or periodic) for all flow directions have been examined and their impact on a medium permeability was observed and documented.

### 4.3. Two-phase flow regimes

Diffuse interface model (DIM) of two-phase pore-scale mass transfer has been developed for simulation of flow in real media. The model is based on Cahn-Hilliard equations (Cahn and Hilliard, 1958) and inherits the principal features of the previously reported one (Bogdanov et al, 2010). The model equations can be found in Appendix below. Note that viewed at micro-scale (=REV-scale), they comprise at least 2 parameters to specify a "space" of the flow regimes (*Re* is fixed!):

$$Ca=\mu_r u_r/\sigma\ ,\ M=\mu_r/\mu_i\ , \qquad (1)$$

where *Ca* and *M* stand for capillary number and viscosity ratio, subscripts "r" and "i" for recovered and injected fluids (typically, oil and water), respectively, other value definitions can be found in Appendix. Detailed analysis of equations (A8) shows that the Cahn number (normally, $Cn >> 1$) and the Peclet number ($Pe >> 1$) might contribute somewhat into flow pattern development. Here (cf. Appendix)

$$Cn=L/\xi\ ,\ Pe=u_r L/M_c \qquad (2)$$

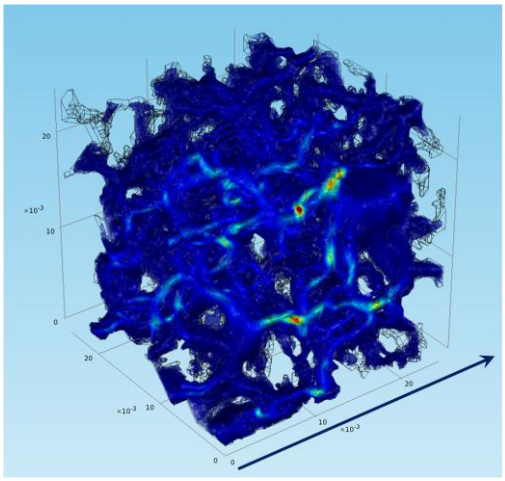

**Figure 5.** Local interstitial velocity field for 1P stationary case: the same 1/8$^{th}$ of original sample like in figures 3, 4.

Recently 2D and 3D numerical analysis demonstrated quite different flow patterns, at least at viscous and capillary dominating regimes (cf. Bogdanov et al, 2010). In particular, the viscous fingering offset at unfavorable viscosity ratio *M* and typical surface tension $\sigma$ is shown in figure 6. Recent example of stable 3D two-phase displacement without gravity in a real medium is illustrated in figure 7.

The locally dominating capillary forces at pore scale are responsible for mass exchange by capillary imbibition which is important mechanism in many practical applications. Modeling this process in its dynamics may

provide better understanding of mass transfer in pores from both qualitative and quantitative viewpoints. The use of realistic geometry of pores becomes evidently one of the key factors for such a modeling.

It seems possible that nothing but complex interplay between pore geometry, fluids wetting and viscous properties, interfacial tension and hydraulic potential contributes equally to the validity of existing theoretical approach. Then any more or less important simplification may lead to a deviation from "equilibrium" and even to degenerate behavior. From this viewpoint the pore scale models can be ultimately useful because of explicit description of all important physical mechanisms.

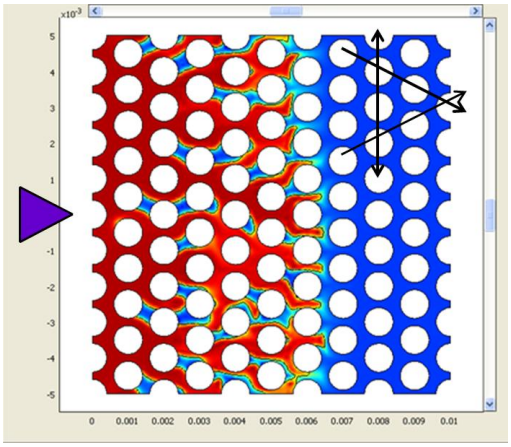

**Figure 6.** Offset of viscous fingering in artificial regular 2D porous medium at $M$=100 with capillary trapping behind leading front advancing to right side (cf. Bogdanov et al, 2010).

## 5. Conclusions and future work

- Promising combination of 3D μCT reconstruction and imaging of the real porous medium (Bentheimer sandstone), the image processing and 3D geometry construction and finally, numerical mesh generation and simulations in COMSOL *Multiphysics* proved to result in a first 3D case study
- Both single- and two-phase flow in real pores has been simulated using incompressible Navier-Stokes and Cahn-Hillird diffuse interface models developed recently for 3D modeling of complex hydrodynamics
- Numerical evaluation of principal physical and geometrical characteristics and transport properties for single- and two-phase flow has been done for synthetic and real samples containing up to few hundreds pores
- The nearest future tasks embrace sensitivity studies for geometrical features and mesh parameters impact on computational results and further computations of two-phase hydromechanical phenomena under local capillary domination which is a natural condition for petroleum applications

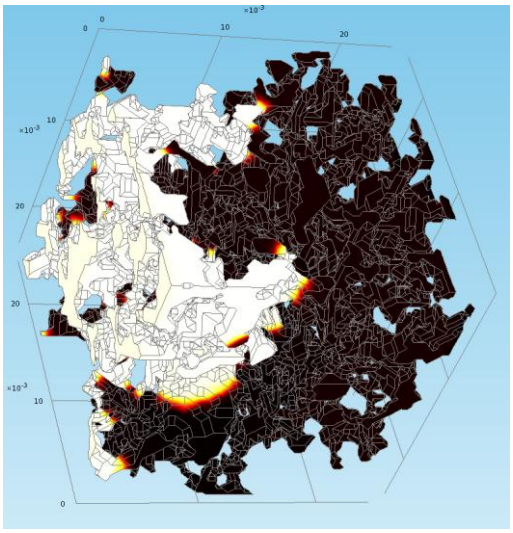

**Figure 7.** Two-phase flow in Bentheimer sandstone: displacement is stable as the injected (white) liquid is more viscous ($M$=0.1) than the displaced (black) one. Flow is directed from left to right.

## 6. References


1. Jacob Bear, *Dynamics of fluids in porous madia*, Dover Publications, Inc., New York (1988)
2. John W. Cahn, John E. Hilliard, Free Energy of a Nonuniform System. I. Interfacial Free Energy, *Journal of Chemical Physics*, 28, No.2, 285-267 (1958)
3. Walter Fourie, Rajab Said, Philippe Young, David L. Barnes, The Simulation of Pore Scale Fluid Flow with Real World Geometries Obtained from X-Ray Computed Tomography, *Proceedings of the Boston COMSOL Conference* (2007)
4. Igor Bogdanov, Sylvain Jardel, Anis Turki, Arjan Kamp, Pore-Scale Phase Field Model of Two-Phase Flow in Porous Medium, *Proceedings of the European COMSOL Conference, Paris* (2010)
5. V. Badalassi, H. Cenciceros and S. Banerjee, Computation of multiphase system with phase field models, *Journal of Computational Physics*, **190**,371-397 (2003).
6. F. Fichot, P. Meekunnasombat, J. Belloni, F. Duval, A. Garcia and M. Quintard, Two-phase

flow in porous media: prediction of pressure drops using a diffuse interface mathematical decription, *Nuclear engineering and design*, **237** 1887-1898 (2007).

## 7. Acknowledgements

TOTAL S.A. is gratefully acknowledged for sponsoring our research projects.

## 8. Appendix. Phase field model for two-phase flow

Below is presented only the brief description of Cahn-Hilliard model. For more details of the theory and its formalism see Badalassi et al. (2003), Fichot et al. (2007). The second gradient theory assumes that free energy of a system is a functional of an order parameter $\varphi$, its gradient $\nabla\varphi$ and the temperature $T$:

$$F = F(\varphi, \nabla\varphi, T). \quad \text{(A1)}$$

In the case of an isothermal binary fluid, a free energy can be defined for flow configurations where the system is not in equilibrium as:

$$F(\varphi, \nabla\varphi) = \alpha \int_{\Omega} f \, dV = \alpha \int_{\Omega} \frac{1}{2}\left(|\nabla\varphi|^2 + g(\varphi)\right) dV \quad \text{(A2)}$$

where $\Omega$ is the region of space occupied by the system and $\varphi$ is a dimensionless phase-field variable which serves to identify the two fluids with volume fraction $(1+\varphi)/2$ and $(1-\varphi)/2$. The chemical potential is defined as:

$$\nu = \alpha \, f'_{\varphi}, \quad \text{(A3)}$$

where $\alpha$ is the mixing energy density [N]. The fourth order partial differential equation describing the evolution of $\varphi$ is the convective Cahn-Hilliard equation:

$$\frac{\partial\varphi}{\partial t} + (\mathbf{u}\cdot\nabla)\,\varphi - \nabla\cdot\left(M(\varphi)\nabla\mu\right) = 0. \quad \text{(A4)}$$

For $g(\varphi)$ a following double potential form is chosen:

$$g(\varphi)=(1/4\xi^2)\cdot(\varphi^2-1)^2, \quad \text{(A5)}$$

where $\xi$ is a capillary width, [m], that scales with the thickness of the diffuse interface. Finally, from (A3) it follows that the chemical potential can be written as:

$$\nu = \frac{\alpha}{\xi^2}\left[\varphi\left(\varphi^2 - 1\right) - \xi^2\nabla^2\varphi\right], \quad \text{(A6)}$$

while for the nonlinear mobility $M$ which is attractive and important for numerical applications, and contributes much to phase separation we choose the following expression (cf. Badalassi et al, 2003):

$$M(\varphi) = M_c\,(1-\gamma\varphi^2)\xi^2 \quad \text{(A7)}$$

where $0 \le \gamma \le 1$. At $\gamma\to 0$ the phase separation dynamics is controlled by bulk diffusion; in the opposite case $\gamma\to 1$, the phase separation dynamics is controlled by interface diffusion. Combining (A4), (A6) and the *modified* Navier-Stokes equations for incompressible fluid, the system of model equations to be solved can be written as:

$$\rho\left(\frac{\partial\mathbf{u}}{\partial t} + (\mathbf{u}\cdot\nabla)\,\mathbf{u}\right) + \nabla p = \nabla\cdot\left[\mu\left(\nabla\mathbf{u} + (\nabla\mathbf{u})^T\right)\right] + \nu\cdot\nabla\varphi$$

$$\nabla\cdot\mathbf{u} = 0$$

+Eq.(A4) +Eq.(A6) (A8)

The equilibrium profile is obtained by minimizing the free-energy functional, with respect to the variations of the function $\varphi$, i.e. simply solving for

$$\nu \equiv \delta F/\delta\varphi = 0,$$

where $F$ is given by (A2). In the case of one-dimensional interface the solution is (cf. Fichot, 2007)

$$\varphi = \pm\tanh[x/(\sqrt{2}\xi)]. \quad \text{(A9)}$$

The equation above is locally true for any particular geometry of the interface in equilibrium, so in all calculations presented in the paper the equation (A9) has been used to give initial phase field over model region. The surface tension is introduced through the integral of the free-energy density across the interface; it can be shown that it relates two above defined model parameters $\alpha$ and $\xi$ via the following relation:

$$\sigma = (2\sqrt{2}/3)\cdot(\alpha/\xi). \quad \text{(A10)}$$

It is practically convenient because easily available surface tension coefficient can substitute α in the model.

The dimensionless formulation defines as usual Reynolds number appeared in the first equation of (A8), but also Cahn number ($Cn=L/\xi$) in the last term of the equation. Beside that the product of the Peclet number ($Pe=u_rL/M_c$) and Cahn number, arises in the last term of the equation (A4), namely, $Pe\cdot Cn^3$. These numbers may be important in definition typical flow regimes in a two-phase case.